Measurement and Analysis of the Capacitance of Charged Objects in a Plasma with Applications to Lorentz-Actuated Spacecraft

Zachary Manchester

May 18, 2010

Abstract

A set of measurement techniques for characterizing laboratory plasmas, as well as measuring the capacitance and current flow associated with a conductor suspended in such plasmas are developed. Emphasis is placed on modeling spacecraft in the ionosphere for engineering applications. Some measurement results are presented for a xenon plasma with a number density of 6.6×10^6 cm^{-3} and temperature of 1320 eV, as well as an analysis of sheath-enhanced capacitance of thin wires with applications for Lorentz-actuated spacecraft.

Contents

List of Figures

1 Introduction

The behavior of plasma around charged objects has important implications for the operation of spacecraft in Earth orbit. Altitudes in excess of a thousand kilometers are permeated by a complex and time varying plasma environment that can impart current to spacecraft, form electrostatic sheaths around them, and build up enormous potentials on electrically conducting surfaces. For the design engineer, knowledge of these effects can not only be used to mitigate damage to spacecraft, but, if properly controlled, may provide a source of propellantless propulsion.

The dynamics of plasmas are very complex and, in spite of decades of research, their behavior can not be fully analytically modeled. Difficulties arise from non-linearity of the governing differential equations, as well as the need to take into account both fluid- and electro-dynamics in a consistent way. To overcome these difficulties numerical methods or empirical measurements must be used. We have taken the second approach, developing an experimental set up and series of measurement techniques by which a laboratory plasma can be generated and characterised. Following this, the sheath thickness, capacitance, and current flow of a conductor suspended in the plasma can be measured as a function of bias potential.

With the knowledge gained from initial experiments, conductors and plasma parameters can be appropriately scaled to model the ionospheric plasma environment for engineering applications. One such application, propellantless spacecraft actuation using the Lorentz force, will be presented and analyzed. Further experiments will allow iterative testing and refinement of this technology.

2 Plasma Theory

Plasmas are ionized gasses. Their physical analysis is complicated by the need to take into account the electrodynamic interactions of their charged constituent particles in addition to the usual kinetic theory of gasses. This section will provide the reader with a survey of basic plasma theory relevant to the discussions in later sections. References will be given throughout for more detailed derivations and further reading.

2.1 Physical Parameters

To describe a plasma in a given region of space, several parameters may be required. We will assume for the remainder of this report that the plasma being treated consists only of electrons and a single ion species. Given these assumptions, the relevant parameters are then the number-density of electrons, n_e and ions, n_i, their masses, m_e and m_i, their charges, q_e and q_i, and their temperatures, T_e and T_i. Here temperature is used as a statistical measure of the average kinetic energy per particle (electron or ion), by way of Boltzmann's constant, K_B, which has units of energy-per-temperature.

An important point to make note of early in this discussion is that masses of the two constituents of plasma, electrons and ions, generally differ by four to five orders of magnitude. For example, the electron mass is $m_e \approx 9.11 \times 10^{-31}$kg, while the mass of a hydrogen ion is $m_H \approx 1.674 \times 10^{-27}$kg and a xenon ion is $m_{Xe} \approx 2.181 \times 10^{-25}$kg. Assuming that a plasma is in thermal equilibrium ($T_e = T_i$) and using Boltzmann's constant ($E = K_B T \propto m\bar{v}^2$) implies that the ratio of average electron speed to average ion speed is given by

$$\frac{\bar{v}_e}{\bar{v}_i} = \sqrt{\frac{m_i}{m_e}} \tag{1}$$

so that the electrons in a plasma, on average, move thousands of times faster than the ions.

2.2 Plasma Oscillations

A useful approximation can be made by assuming that, on short timescales, the ions in a plasma are completely stationary while the electrons are allowed to move in the presence of their combined electric field. This can be visualized as a fixed, homogeneous sheet of ions with charge density $n_i q_i$ contained in the same volume as a mobile homogeneous sheet of electrons with charge density $n_e q_e = -n_i q_i$. If the mobile electron sheet is displaced a small distance x from equilibrium, it will be pulled back by the coulomb force to it's original position. Newton's Second Law gives us

$$\frac{d^2 x}{dt^2} = \frac{E q_e}{m_e} \tag{2}$$

where E is the electric field. Gauss's law gives a way of calculating E from the charge density:

$$\nabla \bullet E = \frac{n_i q_i}{\varepsilon_0} = Constant$$

$$\Rightarrow E = \frac{n_i q_i}{\varepsilon_0} x \tag{3}$$

Substituting eq. (3) into eq. (2) gives a simple harmonic oscillator equation

$$\frac{d^2 x}{dt^2} = \frac{n_i q_i q_e}{\varepsilon_0 m_e} x = -\frac{n_e q_e^2}{\varepsilon_0 m_e} x \tag{4}$$

with frequency

$$\omega_{pe} = \sqrt{\frac{n_e q_e^2}{\varepsilon_0 m_e}} \tag{5}$$

This is known as the plasma electron frequency[9][13], and is seen experimentally as a resonant peak in the frequency response of the plasma to radio frequency excitations.

2.3 Debye Length and Sheaths

An important assumption made in the derivation of the plasma frequency is quasineutrality - the presence of roughly equal amounts of positive and negative charge averaged over the whole extent of the plasma. While quasineutrality is a fundamental defining property of a plasma, it can be violated locally, giving rise to some very important phenomena.

Let us place a negatively charged sphere into a large volume of stationary plasma in thermal equilibrium. Because the charge carriers in plasma are mobile, they will move in the presence of the electric field of the sphere. The charge carriers themselves, however, also contribute to the total electric field in the space surrounding the sphere, so that the potential is not the $\frac{1}{r}$ coulomb potential of a sphere in vacuum. To calculate the potential, we must use Poisson's equation

$$\nabla^2\Phi = \frac{\rho}{\varepsilon_0}$$

which, because of the spherical symmetry of the problem reduces[10] to

$$\frac{1}{r^2}\frac{\partial}{\partial r}\left(r^2\frac{\partial\Phi}{\partial r}\right) = \frac{\rho}{\varepsilon_0} = \frac{nq}{\varepsilon_0} \tag{6}$$

To obtain an expression for the charge density ρ in terms of the potential, we will make use of the Boltzmann distribution[3][7], which gives an expression for the fraction of particles with a given energy E_α.

$$\frac{n_\alpha}{n} = \frac{e^{-E_\alpha/(K_B T)}}{\sum\limits_\alpha e^{-E_\alpha/(K_B T)}} \tag{7}$$

Noting that the bottom of eq. (7) is a constant and substituting in the total energy of an electron (kinetic plus potential) gives

$$n_e \propto e^{-(mv^2/2+q_e\Phi)/(K_B T_e)}$$

Since we only care about the dependence on Φ here, and not the thermal energy of the electrons, we will integrate over all velocities[7] to obtain

$$n_e = n_{e\infty}e^{-q_e\Phi/(K_B T_e)} \tag{8}$$

where $n_{e\infty}$ is the equilibrium electron density before the sphere was inserted into the plasma, and is also the density an infinite distance away from the sphere. If we assume that the potential energy is much smaller than the thermal energy of the electrons ($q_e\Phi \ll K_B T_e$), eq. (8) can be linearized, giving

$$n_e = n_{e\infty}\left(1 - \Phi\left(\frac{q_e}{K_B T_e}\right)\right) \tag{9}$$

Now, substituting into eq. (6) and simplifying gives a linear second-order differential equation for Φ[9]

$$\frac{\partial^2}{\partial r^2}(r\Phi) - \frac{n_{e\infty} q_e^2}{\varepsilon_0 K_B T_e}(r\Phi)$$

with general solution

$$\Phi(r) = \frac{C}{r} e^{-r/\lambda_D}$$

where C is a constant of integration and

$$\lambda_D = \sqrt{\frac{\varepsilon_0 K_B T_e}{n_e q_e^2}} \tag{10}$$

is known as the Debye length. The constant C can be found by enforcing that, in the limit as r approaches zero, the potential must match the standard coulomb potential for a sphere in vacuum, giving

$$\Phi(r) = \frac{1}{4\pi\varepsilon_0} \frac{Q_{sphere}}{r} e^{-r/\lambda_D} \tag{11}$$

where Q_{sphere} is the total charge on the sphere.

The Debye length serves as a sort of "characteristic length scale" for phenomena in a plasma. In the case of our charged sphere, it is the thickness of a concentric region in which electrons are depleted and there are mostly positive ions. Beyond this region, known generally as a sheath, the plasma will effectively shield out the potential of the sphere, limiting the distance over which electrostatic interactions can occur to about a Debye length. This has important implications for both the capacitance of conductors and the ability to collect current from the plasma.

While the Debye length gives a general scale for plasma sheaths, it is at best a rough "order of magnitude" approximation to their true extent. Solving for the actual sheath thickness around a charged surface for any practical situation is an intensive computation that can only be accomplished using numerical methods (see [11] and [5]). For the purposes of this paper, an analytical fit to the data of Laframboise[11] due to Blackwell et. al.[2] will be used.

$$s(\Phi) = \left(2.5 - 1.87 e^{-0.39 r_{sphere}/\lambda_D}\right)\left(\frac{q_e \Phi}{K_B T_e}\right)^{\frac{2}{5}} \lambda_D \tag{12}$$

Note that eq. (12) explicitly includes the sphere's radius, unlike the Debye length, and also that it is only valid for negative biased potentials.

3 Measurement Techniques

Now that we have outlined the basic parameters of interest when studying a plasma, the practical question of how to measure these parameters arises. The two methods presented here make use of the same spherical metal probe inside the plasma chamber, and only differ in the measurement equipment connected via cables outside the chamber and in post-measurement analysis. This has the advantage that both methods may be used sequentially under the same test conditions to check each other. The first method, the plasma impedance probe, is a relatively modern frequency domain approach that is conceptually simple and can give very clear and accurate measurements of sheath thickness, plasma frequency, and electron number density while varying the probe bias potential. The second method, the Langmuir probe, is the classical means of determining the electron temperature and number density of a plasma. While it requires only very simple apparatus and measurements of T_e are fairly straight forward, the analysis needed to extract n_e from Langmuir probe data is difficult and does not produce very precise results. For that reason, we will focus on using the impedance probe to measure sheath thickness and electron number density, while relying on the Langmuir probe for measurements of electron temperature.

3.1 The Plasma Impedance Probe

The impedance probe consists of a single, small, spherical probe suspended in the plasma which is then externally connected via coaxial cable to a network analyzer. It relies on the assumption that the probe-plasma system will respond linearly to small signals at any negative bias voltage, and can thus be modeled as an RLC circuit[2][1].

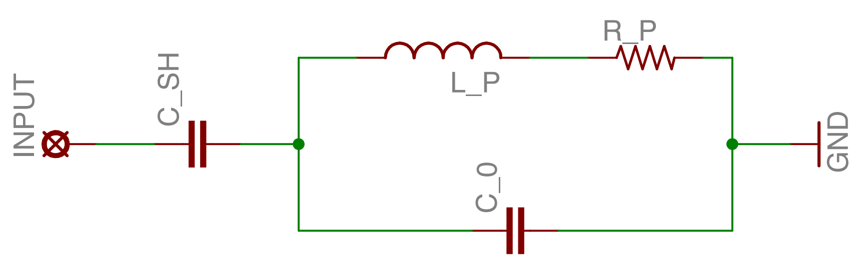

Figure 1: Plasma Impedance Probe Circuit Model

The total impedance of the circuit in figure (1) is

$$Z = \frac{1}{j\omega C_{sh}} + \frac{1}{j\omega C_0 + \frac{1}{R_p + j\omega L_p}} \tag{13}$$

where C_{sh} is the sheath capacitance, C_0 is the vacuum self-capacitance of the spherical probe, and L_p and R_p are the plasma inductance and resistance, respectively. These are given below in terms of other more typical plasma quantities.

$$C_0 = 4\pi\varepsilon_0 r_{sphere}, \quad L_p = \frac{1}{C_0\omega_{pe}^2}, \quad R_p = \nu L_p \tag{14}$$

$$\frac{C_{sh}}{C_0 + C_{sh}} = \frac{r_{sphere} + s}{r_{sphere} + 2s} \tag{15}$$

Note that ν in the expression for R_p is the plasma collision frequency. While the impedance probe method can be used to determine the collision frequency, it is not directly relevant to our goals and it will suffice to say that it does not affect the measurement of ω_{pe} or ω_{sh}.

Some algebraic manipulation of eq. (13) reveals that there are two points at which the reactance (imaginary part of Z) becomes zero. These are resonances, or local extrema in the Impedance vs. frequency plot. One occurs at the plasma electron frequency, given by eq. (5), while the other is known as the sheath resonance, and occurs at a lower frequency given by eq. (16).

$$\omega_{sh} = \omega_{pe}\sqrt{\frac{C_0}{C_{sh} + C_0}} \tag{16}$$

To actually take an impedance measurement, a vector network analyzer (VNA) is connected to the probe and properly calibrated to eliminate errors due to connectors and cabling. The VNA drives the probe with a wide-band signal and produces a plot of the complex reflection coefficient as a function of frequency. Reflection coefficient is defined[8] as

$$\Gamma = \frac{Z - Z_0}{Z + Z_0}$$

where Z_0 is the characteristic impedance of the measuring device and cabling. The impedance of laboratory test equipment and coaxial cable is almost universally 50 ohms, so with this assumption we can easily solve for the probe impedance in terms of the reflection coefficient.

$$Z = 50\left(\frac{1 + \Gamma}{1 - \Gamma}\right) \tag{17}$$

Figure (2) shows a MATLAB simulation of the impedance curve for a 1 cm radius sphere in a plasma with $T_e = 5000$ K and $n_e = 10^7\text{cm}^{-3}$. The code for this simulation is included in appendix A.

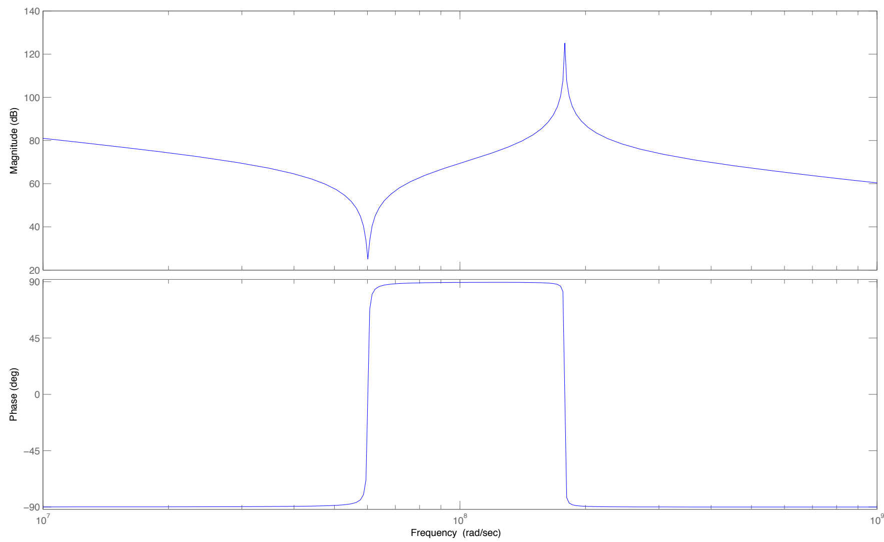

Figure 2: Simulated Probe Impedance

Note that there are two local extrema. The local minimum at around 10 MHz corresponds to the sheath resonance, and is used to extract the sheath capacitance and sheath thickness using eqs. (13) and (15). The local maximum at around 30 MHz is the plasma electron frequency, and can be used to calculate the electron number density using eq. (5). Also, note that both of these extrema in the magnitude plot correspond to zero crossings on the phase plot. This fact is of practical utility when trying to analyze noisy data, as it provides a clear and well-defined point for determining the two frequencies.

3.2 The Langmuir Probe

The Langmuir probe itself is a very simple apparatus. It consists of only a spherical or cylindrical conductor suspended in the plasma and connected externally to a power supply and ammeter. By sweeping the power supply voltage, a plot of current vs. voltage is made (commonly referred to as an I-V curve).

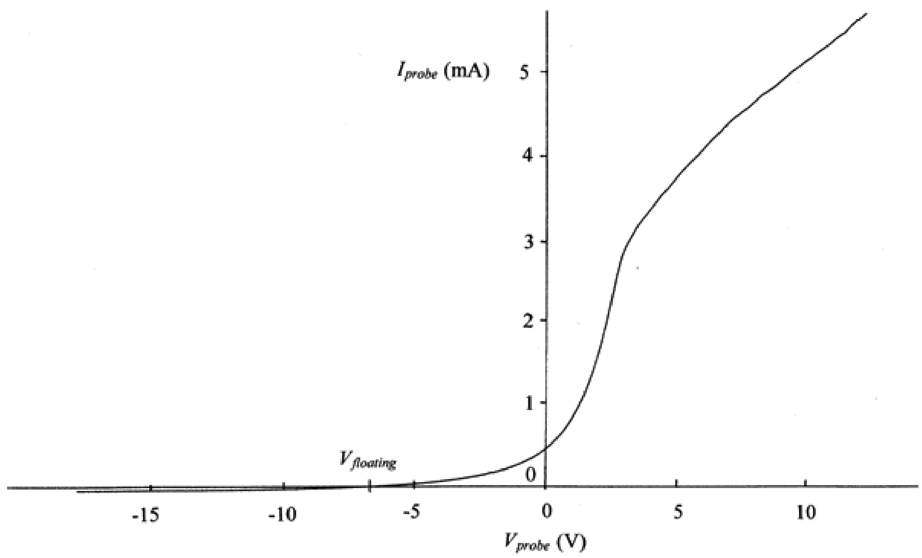

Figure 3: Typical Langmuir Probe I-V Curve

Because of the high relative mobility of the electrons in the plasma, many more electrons will naturally strike the probe than ions. This produces a net negative charge on the probe and a resulting negative floating potential Φ_{fl}. This floating potential, the potential at which no current flows through the probe, is directly related to the electron temperature T_e. Intuitively, it is a potential energy barrier large enough that it cannot be overcome by the thermal energy of most electrons, or $e\Phi_{fl} > K_B T_e$. An explicit expression[4] relating Φ_{fl} to T_e is given by eq. (18).

$$\Phi_{fl} = -\left(\frac{K_b T_e}{2q_e}\right) \ln\left(\frac{m_i}{2\pi m_e}\right) \tag{18}$$

By adjusting the power supply voltage until zero current is displayed on the ammeter, Φ_{fl} can be found and used to solve for T_e. As a practical note, the current displayed by the ammeter is subject to considerable noise, and averaging will greatly improve the ability to take accuracy of measurements.

The determination of electron number density from a Langmuir probe I-V curve is considerably more difficult and error-prone, and will not be treated here since the impedance probe method has proven more reliable. For the interested reader, the original paper by Langmuir and Mott-Smith[12] is still relevant, while the more recent exposition of Chen[4] is more thorough.

4 Experimental Setup

Over a series of experiments, we have refined the application of the Langmuir and impedance probe techniques to the characterization of a xenon plasma and measurements of sheath capacitance for a spherical probe. Our setup consists of a cylindrical vacuum chamber one meter in diameter and one meter in length which is pumped by a mechanical roughing pump and a diffusion pump capable of reaching pressures below 10^{-6} Torr. Inside this chamber are the cathode and heater from an ion thruster, connected using a digital regulator to an external xenon tank. Opposite the cathode, a one inch diameter stainless steel ball is mounted on a stand and connected via a coaxial cable to measuring equipment outside the chamber. This ball may be substituted for other conductor geometries, for example thin wires, though this has yet to be performed.

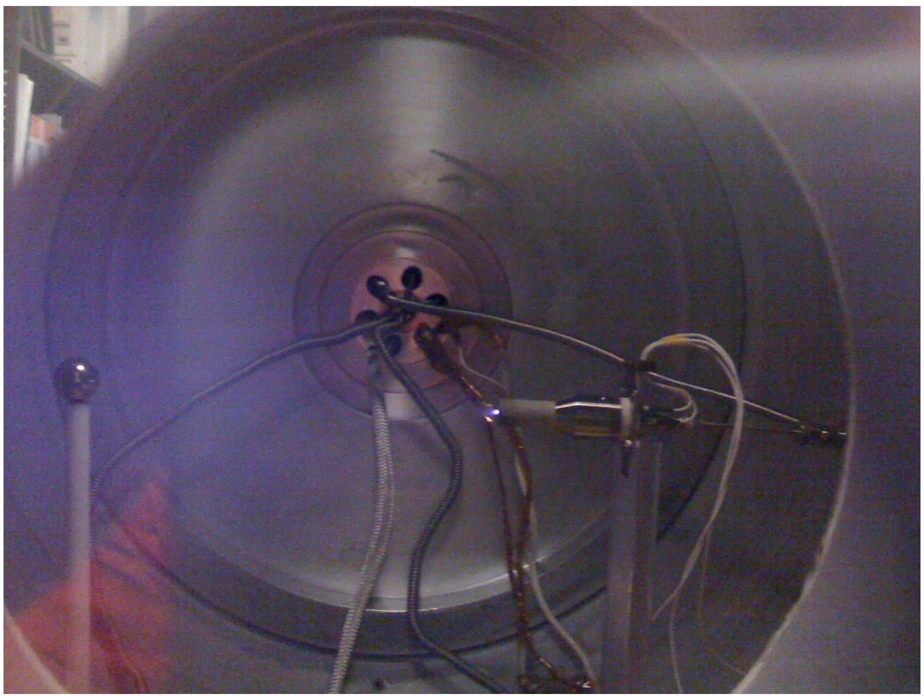

Figure 4: View Inside the Vacuum Chamber

Outside the chamber, the probe is connected in one of two configurations. For I-V measurements, it is connected to a Keithley 6485 picoammeter capable of making current measurements down to 10 nanoamps, then to a bench power supply. For impedance measurements, an HP 8753D vector network analyzer was used. A choke circuit was designed so that the probe could be biased by the bench power supply while simultaneously connected to the VNA.

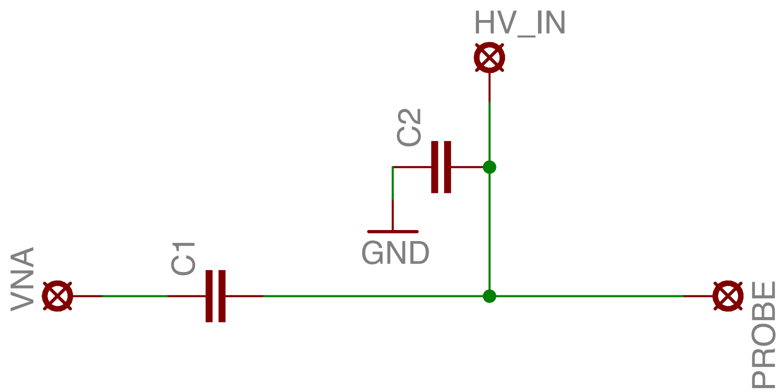

Figure 5: Choke Circuit Diagram

Calibration of the VNA is very important. Before a test run, the chamber must be opened and the sphere removed from its test stand so that the line can be terminated with open circuit, short circuit, and 50 ohm test loads. Data taken by the VNA for these three test loads can then be used to eliminate the effects of the cable and choke circuit so that only the impedance of the sphere and plasma are measured.

After calibration, a typical test run consists of sealing and pumping the vacuum chamber below 10^{-5} Torr, then conditioning and starting the cathode. With the cathode producing plasma, the chamber pressure typically rises to about 10^{-4} Torr. Now, reflection coefficient data may be taken using the VNA while varying probe bias potential, flow rate, and cathode current. Once the desired data is collected using the VNA, the probe may be disconnected and switched to the Langmuir probe configuration using the picoammeter. By varying the probe bias potential while holding the other experimental parameters constant, the floating potential may be found. This can be repeated for all of the parameter sets tested using the VNA so that both temperature and density information is available.

5 Experimental Results

Experimental work has so far been concentrated on achieving reliable plasma characterization and demonstrating the ability to measure sheath thickness for a sphere. Two runs have been performed with the full setup described in the previous section. The first was performed over a very broad frequency range and for many different xenon flow rates and probe bias potentials. Unfortunately, the data form this run was very noisy and not of sufficient resolution to obtain accurate frequency measurements. It did, however allow us to narrow the frequency range of the VNA, and hence achieve much better resolution on the second run.

5.1 Variation in Sheath Thickness with Probe Bias

The first set of measurements were taken at a fixed xenon flow rate of 0.7 sccm and fixed heater and cathode currents of 4 and 0.5 amps respectively. Impedance data was then recorded at increasing probe bias potentials. Figure (6) shows the magnitude and phase of the probe impedance vs. frequency for bias potentials from 0 to -20 volts.

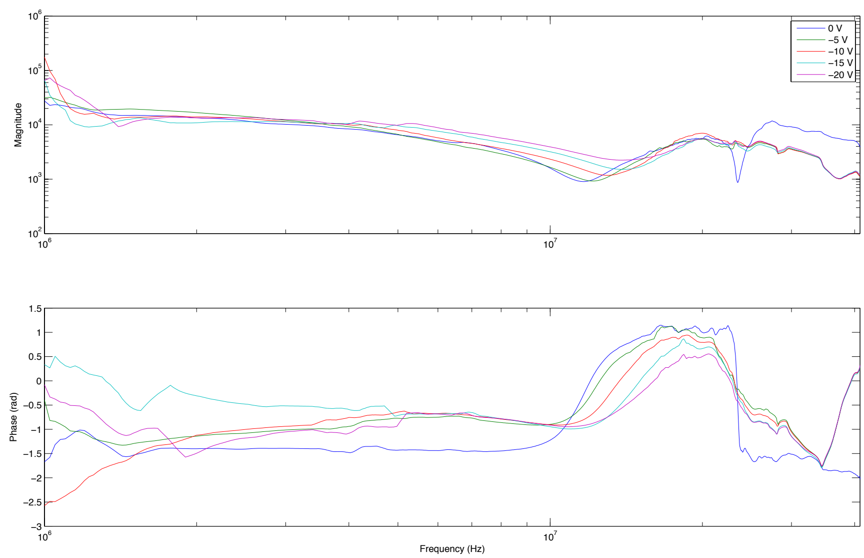

Figure 6: Probe Impedance vs. Frequency for Several Bias Potentials

Note the clear increase in the sheath resonance frequency as bias potential increases. Also, while the local maximum of the plasma resonance isn't particularly apparent in the magnitude plot, the zero crossing in the phase plot associated with it is clearly visible, and remains at the same frequency as the bias is varied. Both of these features are consistent with our theoretical expectations. Using eq. (5), we obtain a value of $6.6{\pm}.1{\times}10^6$ cm^{-3} for n_e. , and using eq. (15) the sheath thickness vs. voltage was calculated and plotted in figure (7).

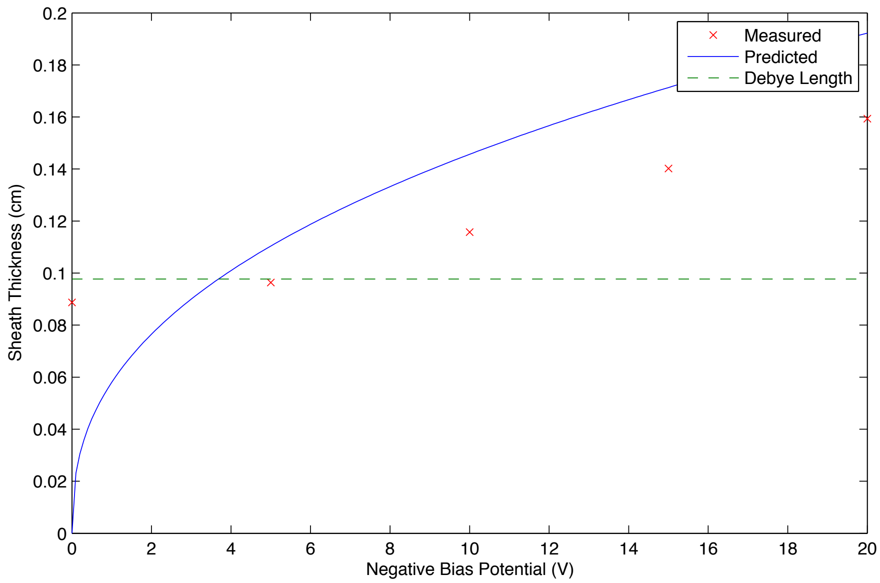

Figure 7: Measured and Predicted Sheath Thickness

The measured sheath thickness is in reasonable agreement with the Debye length at low voltages, as should be expected. It also appears to have a trend similar to that predicted by the Blackwell[2] model of eq. (12) as the bias potential is made more negative (note that the Blackwell model is not valid as Φ approaches zero). While not in complete agreement with the predicted model, the comparison provides evidence that our measurement techniques are sound and that our results are reasonable.

5.2 Variation in Electron Density with Cathode Current

The second set of measurements were taken at a fixed xenon flow rate of 0.7 sccm, heater current at 3 amps, and floating probe potential. The cathode current was then varied above and below its nominal value of .5 amps.

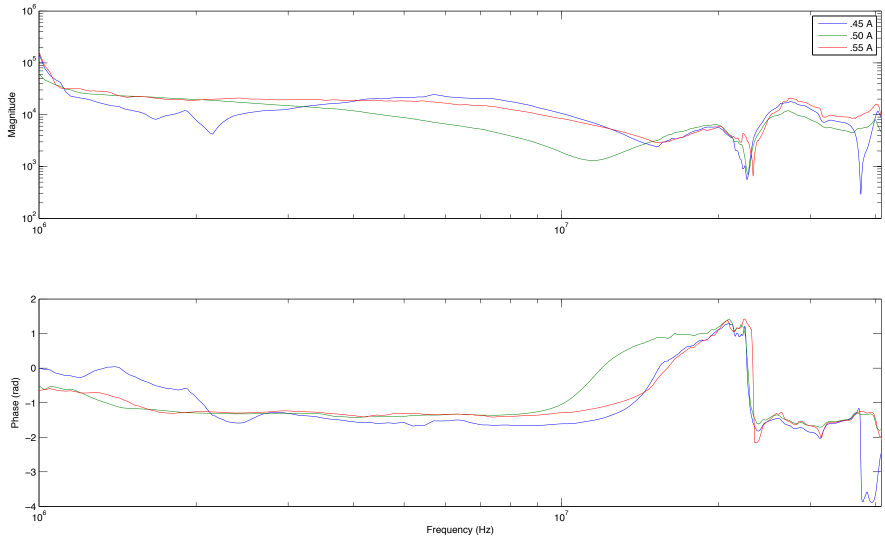

Figure 8: Probe Impedance vs. Frequency for Several Cathode Currents

From the impedance plots, it is clear that the plasma frequency increases with increased cathode current. Making use of eq. (5) again, we find that the electron number density goes from $6.38\times10^6\text{cm}^{-3}$ at .45 A to $6.44\times10^6\text{cm}^{-3}$ at .5 A and $6.72\times10^6\text{cm}^{-3}$ at .55 A. As might be expected, the electron density increases with increased cathode current. This can be explained by the fact that the xenon is not completely ionized when it passes through the cathode, with a sizable portion of the gas leaving as neutral atoms. Increasing the cathode current then increases the proportion of xenon that leaves the cathode ionized, increasing both n_e and n_i.

6 Application to a Lorentz-Actuated Spacecraft

A Lorentz-actuated spacecraft uses the Lorentz force, $F_L = q\underline{v}\times\mathbf{B}$, for propulsion[14]. Assuming an Earth-orbiting spacecraft, let $\underline{v}$ be the spacecraft velocity vector, q the net charge of the spacecraft, and $\mathbf{B}$ the magnetic field of the Earth. In order to alter it's trajectory, the spacecraft must have the ability to alter its charge, which can be accomplished in a number of ways. One method is to apply a potential across two conductors attached to the spacecraft. In the presence of ionospheric plasma, the highly mobile electrons will effectively "ground" the positive conductor, while a sheath will form around the negative conductor. The conductor will have some inherent self-capacitance, as well as some capacitance due to the sheath, enabling it to store charge. The spacecraft as a whole will develop a net negative charge. Two important things to note about this method are that it is only effective for establishing a negative charge, and it requires a power supply to maintain the charge in the presence of current flow from the plasma. To create a practical propulsion system, one would want to maximize stored charge while minimizing power usage.

6.1 Total Charge Storage

To address the first problem of maximizing stored charge, we will analyze two different conductor configurations: a sphere and a long, thin wire. The sphere has a self capacitance C_0 given in eq. (14). In addition, the sheath formed by the plasma effectively creates a larger concentric sphere with opposite charge, enhancing the total capacitance of the system to that of eq. (19).

$$C_{cs} = \frac{4\pi\varepsilon_0 r_{sphere}(r_{sphere} + s)}{s} \tag{19}$$

The same sheath phenomenon happens in the case of a wire, with the sheath forming a coaxial conductor and adding to the total capacitance. In this case, we will assume that the wire is sufficiently long that edge effects can be ignored, so that the capacitance is approximately that given by eq. (20).

$$C_{cw} = \frac{2\pi\varepsilon_0 l}{\ln\left(1 + \frac{s}{r_{wire}}\right)} \tag{20}$$

An ordinary capacitor is a linear device - it stores an amount of charge proportional to the potential across it's terminals, with it's capacitance as the constant of proportionality ($C = \frac{Q}{\Phi}$). The concentric and coaxial sheath capacitors described by eqs. (19) and (20), however, are non-linear, as their capacitance depends on s, which is itself a non-linear function of voltage. In this case, capacitance takes on the stricter definition of $C = \frac{dQ}{d\Phi}$ - the local slope of the charge vs. potential curve. Because of this, to find the total charge stored on a conductor in the plasma, we must numerically integrate the capacitance from 0 to the potential of interest. Figure (9) shows capacitance and total charge on a sphere and a thin wire in a plasma. It demonstrates that the general charging trends are the same for both the sphere and the wire. Also worth noting is that a sphere with a radius of one centimeter has a charge holding ability equal to that of about 15 cm of thin wire.

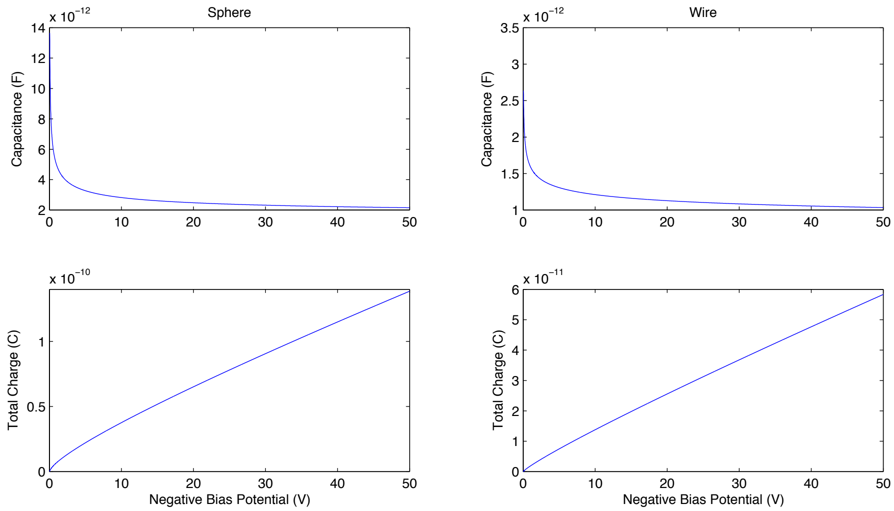

Figure 9: Capacitance and Charge vs. Potential for a Sphere and a Thin Wire

At low potentials - when the sheath thickness is small - the capacitance is indeed greatly enhanced by the sheath to a value an order of magnitude greater than it would be in vacuum. Note, however, that the capacitance asymptotically approaches it's vacuum value as higher potentials are applied. Since total charge is the integral of capacitance, the contribution of the sheath to the total charge carrying ability of the conductor is actually not as large as one might expect - a factor of about $\frac{2}{3}$ increase at 100 volts, and a factor of about $\frac{1}{2}$ at 200 volts.

Above a few tens of volts, the capacitance starts to level off. As a result, the total charge can be approximated quite well above 50 V by an affine function. A good rule of thumb for a sphere in a plasma with parameters similar to those of the ionosphere is that the slope should be equal to about 1.5 times the vacuum capacitance of the conductor, with the constant term approximately equal to the total charge at 10 V.

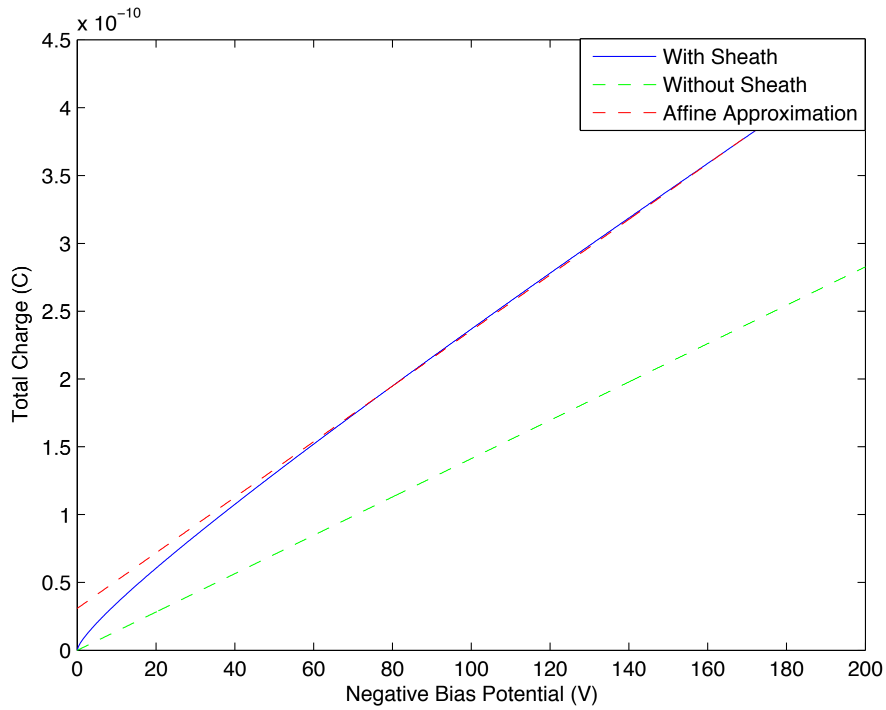

Figure 10: Charge vs. Potential Curves for a Sphere in Plasma and Vacuum

6.2 Power Requirements

Calculating power consumption requires knowledge of the current flow to the conducting surfaces through the plasma. While there are several contributors to the total current, the dominant one for a spacecraft in the ionosphere is thermal current. For the purposes of a bounding estimate, we will ignore all others.

There are two general regimes for thermal current collection by a conductor in a plasma depending on the conductor's size in relation to its sheath. If the conductor is much smaller than the sheath, it is said to be in the "orbital motion limited" or OML regime, while if it is much larger than the sheath, it is said to be in the "sheath limited" regime[15]. For bias voltages between 100 and 1000 volts in ionospheric plasma, the sheath size on the order of 5 cm. At that length scale, the thin wire is squarely in the OML regime, while the sphere radius could be on the same order as the sheath and is not clearly OML or sheath limited. This is a problem, as there is no analytic theory of current collection in a plasma for conductors between the two regimes[4], necessitating further experimental work. For the purposes of this analysis, we will assume that the sphere is also in the OML regime, as this produces higher currents and will give a bounding worst-case.

The random thermal current density to a surface due to a Maxwellian plasma is given by eq. (21)[4].

$$J_{th} = \frac{1}{2} nq \left(\frac{2K_B T}{\pi m} \right) \tag{21}$$

Assuming quasineutrality and thermal equilibrium, this can be written as eq. (22).

$$J_{th} = \frac{1}{2} n_e q_e \left(\frac{2K_B T_e}{\pi m_i} \right) \tag{22}$$

As the potential on the conductor increases, so too does the current. While the I-V relationship is very complicated, for our parameters it can be reasonably approximated by the following formula[4]

$$I_{OML} = A J_{th} F \tag{23}$$

where A is the surface area of the conductor and F is either

$$F_{wire} \approx \frac{2}{\sqrt{\pi}} \eta^{\frac{1}{2}} + e^{\eta} \left(1 - \mathrm{erf}\left(\eta^{\frac{1}{2}}\right)\right) \tag{24}$$

in the case of a long, thin wire or

$$F_{sphere} \approx \eta + 1 \tag{25}$$

in the case of a sphere, where

$$\eta = \frac{q_e \Phi}{K_B T_e}$$

Combining the capacitance and charge models from section 7.1 with this current model, we can study the power required to maintain a given charge for the two different geometries. Since DC power is simply voltage times current, substituting into eq. (23) we obtain the power as a function of potential for both the wire and sphere.

$$P_{wire} = 2\pi r_{wire} l_{wire} \Phi J_{th} F_{wire} \tag{26}$$

$$P_{sphere} = 4\pi r_{sphere}^2 \Phi J_{th} F_{sphere} \tag{27}$$

Looking at eqs. (26)-(27), it becomes clear that the sphere will have much higher power requirements than the wire for the same amount of stored charge. First, the sphere has many orders of magnitude greater area, and second, F_{sphere} goes linearly with potential, while F_{wire} goes approximately as the square root of potential. While the OML current is conservatively high, the difference is likely beyond any modeling uncertainty. Figure (11) shows power consumption vs. stored charge curves for 5, 10, and 20 cm long 22 gauge wires. Note that power consumption varies approximately quadratically with charge, and that power consumption is substantially less with longer wires (or equivalently, a greater number of shorter wires).

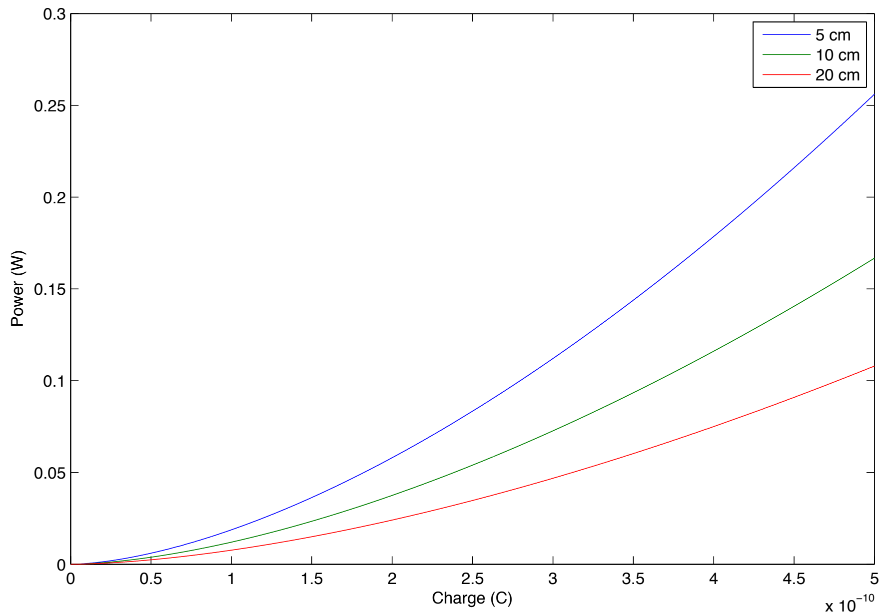

Figure 11: Power Consumption vs. Stored Charge for Different Wire Lengths

7 Conclusion

The experiments performed thus far suggest that the impedance and Langmuir probe techniques and accompanying analysis provide valid measurements of the plasma parameters and sheath capacitance. The eventual goal of these experiments is to be able to evaluate the capacitance and current flow associated with arbitrary conductor geometries in the ionospheric plasma environment. To reach that goal, several more steps must be taken.

First, the dependence of the plasma parameters on variations in the xenon flow rate and cathode and heater currents must be determined. This will involve taking temperature and density measurements while each of those parameters is varied in turn with the other two fixed. This information will allow comparison of the generated plasma to the ionosphere, and will either enable tuning the parameters to more closely match the ionosphere, or provide the information necessary to properly scale experiments.

Second, the portion of xenon that is actually being ionized by the cathode should be determined. This is experimentally accessible through the collision frequency, which appears in the resistance term of the probe impedance and directly determines the width of the peaks in the magnitude plot. This information is again important in determining the degree of fidelity to which the ionosphere can be simulated, and is also important for determining the flow behavior of the plasma as it exits the cathode in a conical jet.

Third, the dependence of the sheath capacitance and probe current on the non-zero flow velocity of the plasma should be determined. The analytic theory of sheath formation assumes a stationary plasma, and exactly what happens in the presence of a flowing plasma is only accessible via experiment or numerical methods (see Choiniere[6]). This is important for evaluating any enhancement of the probe current due to the fluid motion of the plasma itself - known as ram current, another effect that is present for a fast-moving body in the ionosphere.

Lastly, different conductor sizes must be tested. There is evidence that the spherical probe does not fit into existing models for either sheath limited or OML current collection. Testing a range of sizes will allow the development of a new model valid for intermediate size scales, as well as verification and refinement of existing models in the large and small extremes.

While this set of goals encompasses a large and ambitious range of experimental work, the foundations have been successfully laid. Much of the remaining work employs the measurement techniques that have already been developed to test different permutations of plasma parameters and conductor geometries. The knowledge gained will then aid the design of new satellite systems capable of controlling their interactions with the plasma environment.

References

[1] D.D. Blackwell, D.N. Walker, and W.E. Amatucci. Measurement of absolute electron density with a plasma impedance probe. *Review of Scientific Instruments*, 76:023503, 2005.

[2] D.D. Blackwell, D.N. Walker, S.J. Messer, and W.E. Amatucci. Characteristics of the plasma impedance probe with constant bias. *Physics of Plasmas*, 12:093510, 2005.

[3] R. Bowley, M. Sanchez, and R.S. Knox. *Introductory Statistical Mechanics*. Clarendon Press Oxford, 1999.

[4] Francis F. Chen. Electric probes. *Plasma Diagnostic Techniques, ed. by RH Huddlestone, SL Leonard*, 4, 1965.

[5] E. Choiniere. Theory and experimental evaluation of a consistent steady-state kinetic model for two-dimensional conductive structures in ionospheric plasmas with application to bare electrodynamic tethers in space. 2004.

[6] E. Choiniere and B.E. Gilchrist. Self-consistent 2-d kinetic simulations of high-voltage plasma sheaths surrounding ion-attracting conductive cylinders in flowing plasmas. *IEEE Transactions on Plasma Science*, 35(1):7–22, 2007.

[7] RJ Goldston and P.H. Rutherford. *Introduction to plasma physics*. Taylor & Francis, 1995.

[8] D.J. Griffiths and C. Inglefield. *Introduction to electrodynamics*. Prentice Hall New Jersey;, 1999.

[9] D.A. Gurnett and A. Bhattacharjee. *Introduction to plasma physics: with space and laboratory applications*. Cambridge Univ Pr, 2005.

[10] JD Huba. *NRL Plasma Formulary*. Naval Research Lab, Plasma Physics Division, Washington, DC, 2009.

[11] J.G. Laframboise. Theory of spherical and cylindrical langmuir probes in a collisionless, maxwellian plasma at rest. 1966.

[12] HM Mott-Smith and I. Langmuir. The theory of collectors in gaseous discharges. *Physical review*, 28(4):727–763, 1926.

[13] D.R. Nicholson. *Introduction to Plasma Theory*. Wiley New York, 1983.

[14] M.A. Peck. Prospects and challenges for lorentz-augmented orbits. In *AIAA Guidance, Navigation and Control Conference, San Francisco, CA*, pages 15–18, 2005.

[15] E.C. Whipple. Current collection from an unmagnetized plasma: A tutorial. In *In NASA, Marshall Space Flight Center, Current Collection from Space Plasmas p 1-12 (SEE N91-17713 09-75)*, pages 1–12, 1990.

A Impedance Probe Simulation Code

```
%------------------ Experimental Parameters ------------------
n_e = 5.0e6; %Number Density 1.07e7 (cm^-3)
T_e = 1500; %Electron temperature 4840 (K)
rho = 1; %Probe radius 1.27(cm)
V = -1.0; %Probe bias (V)

%-------------------- Physical Constants --------------------
ep_0 = 8.854187817e-12; %Vacuum Permitivity (F/m)
e = -1.602176487e-19; %Electron charge (C)
m_e = 9.10938215e-31; %Electron mass (kg)
K_b = 1.3806504e-23; %Boltzmann's Constant (J/K)
K_ev = 8.617343e-5; %Boltzmann's Constant (eV/K)

%-------------------- Plasma Quantities --------------------
%Debye length (cm)
lambda = sqrt(ep_0*K_b/(e^2))*sqrt(T_e/(n_e*100^3))*100

%Plasma frequency (rad/sec)
omega_pe = sqrt(e^2/(m_e*ep_0))*sqrt(n_e*100^3);

f_pe = omega_pe/(2*pi) %Plasma frequency (Hz)
N_d = n_e*lambda^3; %Electrons in one Debye cube
nu_ei = 500000; %Collision frequency (Hz)

%Sheath thickness (Blackwell) (cm)
s = (2.5 - 1.87*exp(-0.39*rho/lambda))*(e*V/(K_b*T_e))^(2/5)*lambda

%---------------------- Circuit Model ----------------------
%Capacitance of metal sphere (Farads)
C_0 = 4*pi*ep_0*(rho/100);

rsr2s = (rho+s)/(rho+2*s);
%Capacitance of sheath (Farads)
C_sh = C_0*(rsr2s/(1-rsr2s));

%Bulk plasma inductance (Henries)
L_p = 1/(C_0*omega_pe^2);

R_p = nu_ei*L_p; %Bulk plasma resistance (ohms)

%Sheath resonance frequency (rad/sec)
omega_sh = omega_pe*sqrt(C_0/(C_sh+C_0));
```

```
f_sh = omega_sh/(2*pi) %Sheath resonance frequency (Hz)
Z_sh = tf([1],[C_sh 0]); %Sheath impedance (ohms)
Z_c0 = tf([1],[C_0 0]); %Metal sphere impedance (ohms)

%Bulk plasma impedance (ohms)
Z_tank = tf([L_p R_p], [1]);

%Total impedance (ohms)
Z_total = Z_sh + 1/(1/Z_c0 + 1/Z_tank);

%Reflection Coefficient
Gamma = (Z_total - 50)/(Z_total + 50);

figure(1)
%subplot(121);
bode(Z_total);
%subplot(122);
bode(Gamma);
```

B Capacitance and Total Charge Code

```
function Ctotal = Ctotal(V)

%----------------------- Experimental Parameters -----------------------
n_e = 6.5885e+06; %Number Density (cm^-3)
T_e = 1.3202e+03; %Electron temperature (K)
rho = 1.27; %Probe radius (cm)
l = 5; %Wire length (cm)
r = .0332; %Wire radius (cm) (this is 22 guage)

%------------------------- Physical Constants -------------------------
ep_0 = 8.854187817e-12; %Vacuum Permitivity (F/m)
e = -1.602176487e-19; %Electron charge (C)
m_e = 9.10938215e-31; %Electron mass (kg)
K_b = 1.3806504e-23; %Boltzmann's Constant (J/K)

%---------------------- Capacitance Calculations ----------------------
lambda = sqrt(ep_0*K_b/(e^2))*sqrt(T_e/(n_e*100^3))*100; %Debye length (cm)
% Sheath thickness (Blackwell)
s = (2.5 - 1.87*exp(-0.39*rho/lambda)).*(e.*V./(K_b*T_e)).^(2/5).*lambda; % (cm)

if s < lambda
    s = lambda;
end

Ctotal = 4*pi*ep_0*(rho/100).*((rho + s)./s); %Concentric spheres
%Ctotal = (2*pi*ep_0*(l/100))./log((r+s)./r); %Coaxial cylinders

end
```

```
function Qtotal = Qtotal(V)

%Integrate the Capacitance (C = dQ/dV) to find total Q
Qtotal = quad(@Ctotal, V, 0);

end
```